



Angular and Thermal Dependence of Defect Modes in Si-Based One-dimensional Photonic Crystal

Kamal Deep Jindal¹, Arun Kumar², Vipin Kumar^{3*},
Bhuvneshwer Suthar⁴ and Khundrakpam Saratchandra Singh³

¹Department of Physics, Venkateshwara University, Gajraula (J.P. Nagar), India.

²AITTM, Amity University, NOIDA, India.

³Department of Physics, Digamber Jain (P.G.) College, Baraut 250611, India.

⁴Department of Physics, Govt. College of Engineering & Technology, Bikaner 334004, India.

Authors' contributions

This work was carried out in collaboration between all authors. Authors KDJ and VK contributed to the preliminary computer programming and prepared the first draft. Author BS helped in designing the all Figures in the present form. Author KSS being the guide to author AK co-wrote the paper and finalized the paper in the present form. All authors read and approved the final manuscript.

Research Article

Received 13th June 2013
Accepted 27th July 2013
Published 7th October 2013

ABSTRACT

The effect of temperature and angle of incidence on defect modes in one-dimensional photonic crystal structure for TE and TM polarizations has been studied in 5-9 μ m wavelength region. A symmetric Si/air multilayer system, [(Si/air)⁵Si(air/Si)⁵] has been considered in this communication. The refractive index of Si layer is taken to be dependent on temperature and wavelength simultaneously. As the refractive index of Si layer is a function of temperature of medium as well as the wavelength of incident light, this results to the tuning of defect modes. As defect modes are function of temperature, one can tune the defect modes to desired wavelength. The defects modes can also be tuned by angle of incidence for both polarizations. This type of tunable filter may be used as thermal sensing optical device etc.

Keywords: photonic bandgap materials; multilayers; defects; optical properties.

*Corresponding author: Email: vrpcommon@gmail.com;

1. INTRODUCTION

During the last two and a half decades, photonic crystals (PCs), in particular, photonic band gap (PBG) materials have become area of interest of considerable number of researchers leading to various potential applications of photonic crystal based devices [1-4]. The main attraction of PBGs is the existence of forbidden band gaps in their transmission spectra. Band gaps in a PC are analogous to the electronic band gap in a solid as there is a similarity between the structural periodicity of a PC and the periodic potential energy in a solid. Of the various applications of PCs, some of important applications are trapping of light, optical switches, resonance cavities and waveguides [5-8]. Recently, many studies have been focusing on changing the parameters in a PC to fabricate devices with modulation capability. For example, a slight change of the dielectric constant can be applied to optical switching devices [9].

In addition to the existence of wide band gaps in some properly designed PCs, the feature of a tunability of PBGs in PCs attracts the attention of investigators in recent years. PBGs can be tuned by means of some external agents. For instance, it can be changed with the variation of operating temperature and we call it T-tuning [10]. A superconductor/dielectric PC belongs to this type because of the dependence of the properties of such PCs on temperature. This happens because of the temperature-dependent London penetration length in the superconducting materials [11-13]. Using a liquid crystal as one of the constituents in a PC, the T-tuning optical response is also obtainable [14]. Recently, PCs containing semiconductor as one of the constituents have also been investigated by many researchers. PCs with intrinsic semiconductor belong to T-tuning devices because the dielectric constant of an intrinsic semiconductor is strongly dependent on temperature [15].

The idea of doped PCs comes from the analogy between electromagnetism and solid state physics; and this drew the attention of some investigators to the study of band structures of periodic materials and further to the possibility of the occurrence of localized modes in the band gap when a defect is introduced in the lattice. These defect-enhanced structures are called doped photonic crystals and present some resonant transmittance peaks in the photonic band gap corresponding to the occurrence of the localized states, which may be attributed due to the change of the interference behavior of the incident waves [16]. The defect can be introduced into perfect PCs by changing the thickness of a layer [17], inserting another dielectric into the structure [18,19] and removing any part of the dielectric from the geometry [20,21].

The introduction of the defect states within PCs has been perceived as a new dimension in the study of photonic crystals, especially in 2D and 3D PCs due to numerous possible applications that can be achieved by using them. In 2D or 3D PCs, it has also been known that a point defect can act as a micro cavity [22], a line defect like a waveguide [23], and a planar defect like a perfect mirror [24]. Similar to 2D or 3D PCs, the introduction of the defect layers in 1D PCs can also create localized defect modes within the one-dimensional PBG materials. Due to the simplicity in 1D PCs fabrications over 2D and 3D, the defect mode can be easily introduced within 1D PCs for various applications such as in the designing of TE/TM filters and splitters [25], in the fabrication of lasers [26], and in diodes for electromagnetic wave [27].

Although a few works on the temperature dependence of defect modes in one dimensional photonic crystal has been reported by Hung et al [28] and Chang et al [29], the first work was in the visible region whereas second one was in the 40-70 μm wavelength domain. However,

the present work deals with the study of 1DPC in the 5-9 μ m wavelength region and this range is of particular importance in metrology and other applications. Also, we have considered the behavior of defect mode in 1DPC at higher temperature range up to 900K.

We consider semiconductor media as one of the constituents of a one dimensional photonic crystal, since the dielectric property of intrinsic semiconductors depends not only on temperature but also on wavelength. Here, we consider the Si/air multilayer system with a Si layer as a defect in the middle of the structure. In this communication, thermal tuning of defect modes by changing the temperature and the angle of incidence for a one-dimensional crystal structure with a defect has been studied. The refractive index of air is independent of temperature and wavelength. But the refractive index of silicon layer is taken as a function of temperature and wavelength [15]. Therefore, this study may be considered to be physically more realistic.

2. THEORETICAL MODEL

The schematic representation of one-dimensional photonic crystal with a single defect is shown in Fig. 1.

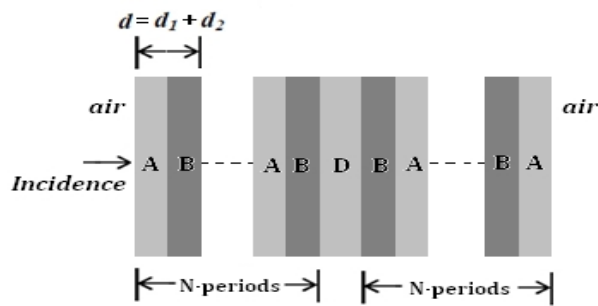


Fig. 1. Schematic diagram of 1-D photonic crystal with defect

We consider air/(AB)^ND(BA)^N/air, in which A and B represents the high and low refractive index materials, and D is the defect layer. To compute the defect mode in the transmission spectrum, we employ the transfer matrix method (TMM) [30,31]. In this method, the transfer matrix for each layer can be written as

$$M_j = Z_j P_j Z_j^{-1}; \tag{1}$$

where, j stands for A, B or D layers and Z_j and P_j are called the dynamical matrix and the propagation matrix respectively. The dynamical matrices are given by the following equations

$$Z_j = \begin{pmatrix} 1 & 1 \\ n_j \cos \theta_j & -n_j \cos \theta_j \end{pmatrix} \text{ for TE mode} \tag{2}$$

where, θ_j is the angle of incidence in the corresponding layer and j stands for A, B or D layers.

and $Z_j = \begin{pmatrix} \cos \theta_j & \cos \theta_j \\ n_j & -n_j \end{pmatrix}$ for TM mode (3)

Also, the propagation matrix P_j can be defined as

$$P_j = \begin{pmatrix} e^{i\delta_j} & 0 \\ 0 & e^{-i\delta_j} \end{pmatrix} \tag{4}$$

where the phase is written as

$$\delta_j = \frac{2\pi d_j}{\lambda} n_j \cos \theta_j \tag{5}$$

The transfer matrix, for the structure embedded in air, air/(AB)^ND(BA)^N/air can be written as

$$M = \begin{pmatrix} M_{11} & M_{12} \\ M_{21} & M_{22} \end{pmatrix} = Z_0^{-1} (M_A M_B)^N M_D (M_A M_B)^N Z_0 \tag{6}$$

where, Z_0 is called the dynamical matrix for air.

The reflection and transmission coefficients can be written as

$$r = \frac{(M_{11} + q_f M_{12})q_i - (M_{21} + q_f M_{22})}{(M_{11} + q_f M_{12})q_i + (M_{21} + q_f M_{22})} \tag{7}$$

And $t = \frac{2q_i}{(M_{11} + q_f M_{12})q_i + (M_{21} + q_f M_{22})}$ (8)

where $q_{i,f} = n_{i,f} \cos \theta_{i,f}$ for TE wave and $q_{i,f} = (\cos \theta_{i,f}) / n_{i,f}$ for TM wave, where the subscripts i and f correspond to the quantities respectively in the medium of incidence and the medium of emergence. In our calculations, we consider both the media to be air. Whereas, the reflectance and the transmittance of the structure are given by

$$R = |r|^2 \quad \text{and} \quad T = \frac{q_f}{q_i} |t|^2 \tag{9}$$

2.1 Proposed Structure and Structural Parameters

We choose Si as the material for the regions A and D, air for layers B and N=5 in Fig. 1. So, the proposed structure will be [(Si/air)⁵Si(air/Si)⁵]. We take silicon and air as the high and the low refractive index materials respectively and an additional silicon layer (D) as the defect layer.

The refractive index of air is independent of temperature and wavelength. But the refractive index of silicon layer is taken as a function of both wavelength and temperature. The refractive index of Silicon (Si) in the ranges 1.2 to 14 μm and 293-900K can be expressed as a function of both the wavelength and temperature as [15].

$$n^2(\lambda, T) = \varepsilon(T) + \frac{e^{-3\Delta L(T)/L_{293}}}{\lambda^2} (0.8948 + 4.3977 \times 10^{-4} T + 7.3835 \times 10^{-8} T^2) \quad (10)$$

where

$$\varepsilon(T) = 11.4445 + 2.7739 \times 10^{-4} T + 1.7050 \times 10^{-6} T^2 - 8.1347 \times 10^{-10} T^3$$

and

$$\frac{\Delta L(T)}{L_{293}} = -0.00071 + 1.887 \times 10^{-6} T + 1.934 \times 10^{-9} T^2 - 4.554 \times 10^{-13} T^3 \quad \text{for } 293\text{K} \leq T \leq 900\text{K}$$

Where, $\frac{\Delta L(T)}{L_{293}}$ is the thermal expansion coefficient of the Si layer. The geometrical

parameters are so chosen that the thicknesses of high and low refractive index materials are same at 293K temperature i.e. $d_1 = d_2 = 1500\text{nm}$ and the thickness of defect layer is taken 2000nm. Thermal expansion coefficient for silicon is taken to be $2.6 \times 10^{-6}/\text{K}$ and melting point is 1685K [32]. In the thickness of silicon layers, the effect of thermal expansion has been taken account of by applying the following equation [33]:

$$d_1(T) = d_{293} \left(1 + \frac{\Delta L(T)}{L_{293}} \right) \quad (11)$$

Where, d_{293} is the thickness of the Si layer at 293K. The absorption in silicon for the particular range of wavelength considered in our calculation is considerably small; and hence for the sake of simplicity and for an approximate calculation of the transmittance of the structure, we may safely ignore the effect of absorption in silicon layers [30].

3. RESULTS AND DISCUSSION

In this section, we present the transmission spectra using equation (9) for defect modes in one dimensional photonic crystal with defect. The plot of the refractive index as the function of wavelength and temperature is shown in Fig. 2. From Fig. 2, it is clear that the refractive index of silicon decreases with the increase in wavelength and increases with increase in temperature. The increase in refractive index is 0.02/100K and the decrease in refractive index is 0.001/ μm . Therefore the refractive index contrast increases with temperature.

The transmittance spectra of the ideal PC (Si/air)¹⁰ at 300K and 900K temperature are shown in Fig. 3. Our purpose is to produce the defect mode in these spectra, which can be tuned by the variation of temperature and angle of incidence. The transmittance spectra for the TE and the TM modes of polarization of the symmetric PC [(Si/air)⁵Si(air/Si)⁵] with a defect at the middle at temperatures 300K and 900K are shown in Figs. 4 and 5 respectively. The data corresponding to defect modes are tabulated in Table 1. We choose 0°, 30° and 60° as the angle of incidence for both cases. Due to the Si defect layer, a defect mode is created at 6.733 μm wavelength at 300K and normal incidence.

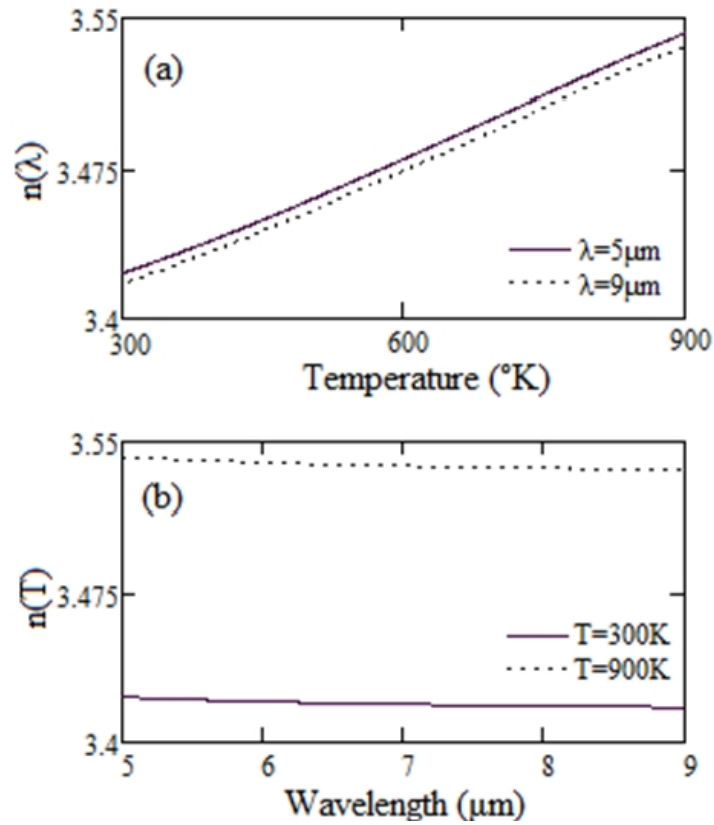


Fig. 2. Variation of refractive index of Si (a) with temperature (at constant wavelength) (b) with wavelength (at constant temperature)

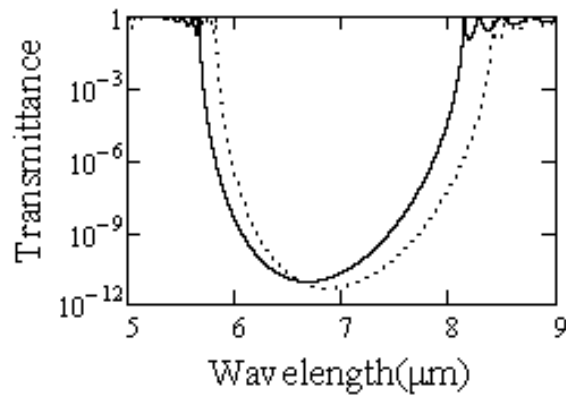


Fig. 3. Transmission spectra without defect At $T = 300\text{k}$ (solid line) and $T = 900\text{k}$ (Dotted)

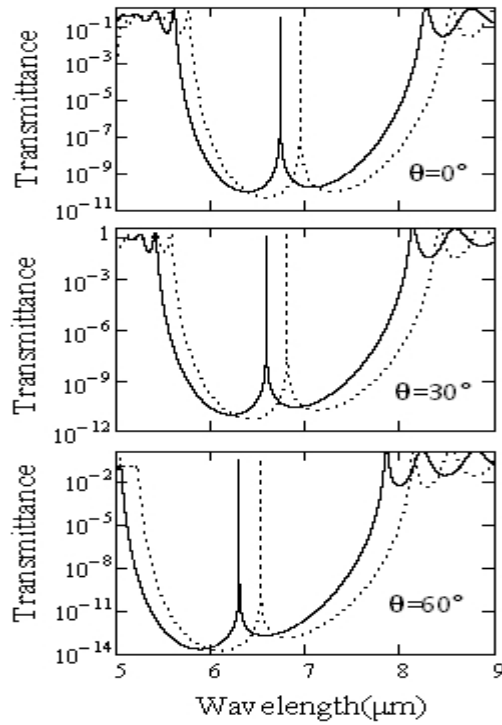


Fig. 4. Transmission spectra of proposed structure for TE-mode of polarization at T=300K(Solid line) and T=900K(dotted line)

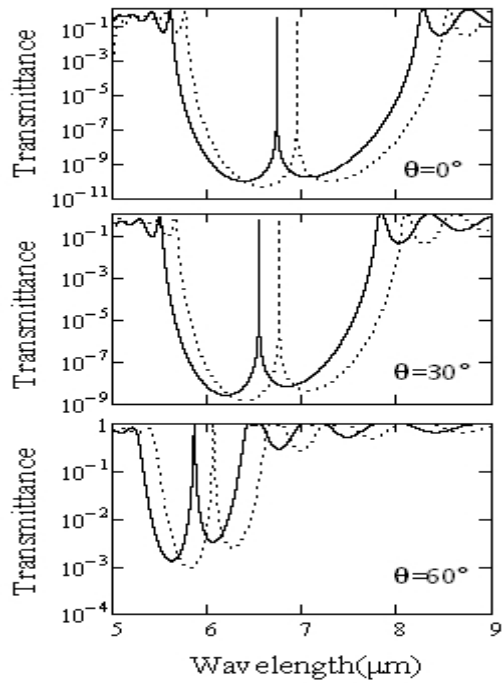


Fig. 5. Transmission spectra of proposed structure for TM-mode of polarization at T=300K (Solid line) and T=900K (dotted line)

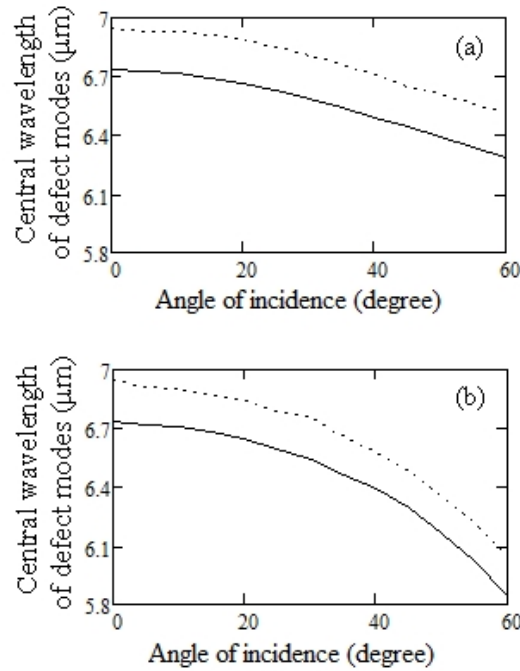


Fig. 6. Variation of central wavelength of the defect modes with angle of incidence (a) TE-mode of polarization (b) TM-mode of polarization at T=300K (Solid line) and T=900K (dotted line)

At normal incidence, the defect modes for both TE and TM polarization modes are found at the same wavelength. This defect mode can be tuned by variation in temperature and angle of incidence. The wavelengths like 1.3 micron and 1.55 micron correspond to low loss optical windows in the optical fiber communication. Whereas, the wavelength corresponding to defect modes in our calculation falls in the region of wavelength (6.0-7.0 μm); and it has potential applications in metrology and in other fields. From Fig. 4 and Table 1, it is clear that the transmission peaks are centered at 6.733 μm and 6.946 μm corresponding to temperatures at 300K and 900K respectively at normal incidence. Therefore, as we increase the temperature, the defect mode of transmission shifts towards the longer wavelength region both for TE and TM modes. The dependence of defect modes on temperature is due to the two factors. First, it is the thermal expansion of defect Si layer and second, due to the dependence of refractive index of silicon on temperature as given in equation (10). The shifting behavior can be explained by using the phase equation (5). According to this phase equation, as $n(\lambda, T)$ increases with temperature, the wavelength must increase accordingly to keep the phase δ unchanged.

Table 1. Central wavelength of defect modes (in μm) at various angles of incidence

Angle of incidence	Central wavelength in μm (TE Mode)		Central wavelength in μm (TM Mode)	
	300K	900K	300K	900K
0°	6.733	6.946	6.733	6.946
30°	6.587	6.804	6.545	6.757
60°	6.282	6.529	6.875	6.085

On the other hand, the effect of angle of incidence on the defect mode is also shown in the figures and Table 1 discussed above. As we increase the angle of incidence, the defect mode shifts towards the lower wavelength region. The shifting of defect modes with angle of incidence can be explained by using the phase equation (5). According to this phase equation, as we increase the angle of incidence, the value of the cosine function on right hand side decreases. Therefore, the wavelength must decrease accordingly to keep the phase δ unchanged. The variation of central wavelength of defect modes with angle of incidence is shown in Fig. 6. It is found that the central wavelength of defect modes does not change linearly with angle. But the difference between the wavelengths corresponding to the defect mode peaks is the same for each angle of incidence. This behavior is helpful in tuning the defect modes.

The variation of central wavelength of defect modes with temperature is shown in Fig. 7. It is found that the central wavelength of defect modes varies approximately linearly with temperature. So, we can use the proposed structure as temperature sensing device, narrow band optical filter, etc. From Fig. 6 and Table 1, it is clearly seen that the defect mode peak shifts towards the longer wavelength region. Also, it is clear that the average change in wavelength of defect modes are $0.038 \mu\text{m}/100\text{K}$ and $0.032 \mu\text{m}/100\text{K}$ for TE and TM mode respectively.

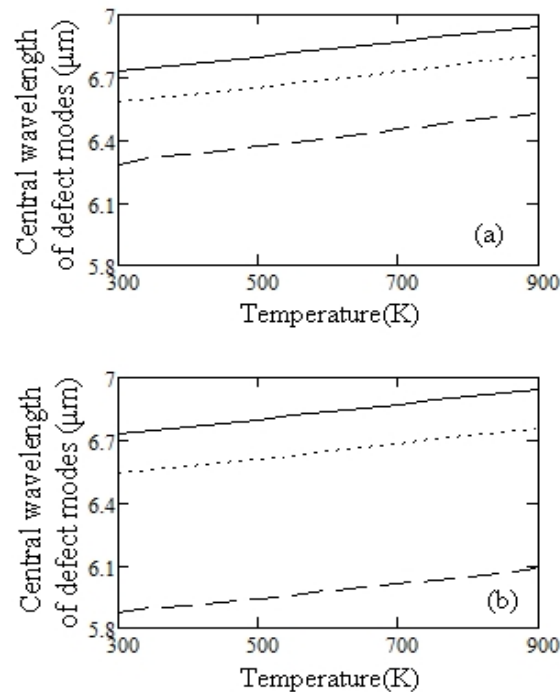


Fig. 7. Variation of central wavelength of the defect modes with temperature (a) TE-mode of polarization (b) TM-mode of polarization at $\theta=0^\circ$ (Solid line), $\theta=30^\circ$ (dotted line) and $\theta=60^\circ$ (dashed line)

From Fig. 4 and Table 1, it is clear that the transmission peaks are centered at $6.733\mu\text{m}$ and $6.946\mu\text{m}$ corresponding to temperatures at 300K and 900K respectively at normal incidence.

Therefore, as we increase the temperature, the defect mode of transmission shifts towards the higher wavelength region both for TE and TM modes

CONCLUSIONS

The effect of the temperature on the defect modes in transmission spectra has been investigated. The refractive index of silicon layers is taken as a function of temperature and wavelength both. Therefore, this study may be considered to be physically more realistic. We can use the proposed structure as temperature sensing device, narrow band optical filter, wavelength division demultiplexer and in metrology.

ACKNOWLEDGEMENTS

The authors are thankful to Prof S.P. Ojha for his kind cooperation and critical comments.

COMPETING INTERESTS

Authors have declared that no competing interests exist.

REFERENCES

1. Yablonovitch E. Inhibited spontaneous emission in solid-state physics and electronics. *Phys Rev Lett.* 1987;58:2059-2062.
2. John S. Strong localization of photons in certain disordered dielectric superlattices. *Phys Rev Lett.* 1987;58:2486-2489.
3. Joannopoulos JD, Meade RD, Winn JN. *Photonic Crystals*, Princeton University Press, Princeton; 1995.
4. Soukoulis CM. *Photonic Band Gap Materials*, NATO ASI, Kluwer Academic Publishers, Dordrecht; 1986.
5. Kumar A, Kumar V, Suthar B, Ojha M, Singh KS, Ojha SP. Trapping of light in non-linear photonic crystal. *IEEE: Photon Technol Lett.* 2013;25(3):279-282.
6. Leonard SW, Driel HV, Schilling J, Wehrspohn. Ultrafast band-edge tuning of a two-dimensional silicon photonic crystal via free-carrier injection. *Phys Rev B.* 2002;66:161102.
7. Kumar V, Singh KS, Singh SK, Ojha SP. Broadening of omnidirectional photonic band gap in Si-based one-dimensional photonic crystals. *Prog Electromagn Res M.* 2010;14:101-111.
8. Lin SY, Chow E, Hietala V, Villeneuve PR, Joannopoulos JD. Experimental demonstration of guiding and bending of electromagnetic waves in a photonic crystal. *Science.* 1998;282:274-276.
9. Wang X, Kempa K, Ren ZF, Kimball B. Rapid photon flux switching in two-dimensional photonic crystals. *Appl Phys Lett.* 2004;84:1817-1819.
10. Kumar A, Kumar V, Suthar B, Bhargava A, Singh KS, Ojha SP. Wide range temperature sensors based on one-dimensional photonic crystal with a single defect. *Int J Micro Sci Technol.* 2012;Article ID 18279 3:5 Pages.
11. Bermann OL, Lozovik YE, Eiderman SL, Coalson RD. Superconducting photonic crystals: Numerical calculations of the band structure. *Phys Rev B.* 2006;74:092505.
12. Takeda H, Yoshino K. Tunable photonic band schemes in two-dimensional photonic crystals composed of copper oxide high-temperature superconductors. *Phys Rev B.* 2005;67:245109.

13. Lin WH, Wu CJ, Yang TJ, Chang SJ. Terahertz multichanneled filter in a superconducting photonic crystal. *Optics Express*. 2010;18:27155.
14. Halevi P, Reyes-Avendano JA, Reyes-Cervantes JA. Electrically tuned phase transition and band structure in a liquid-crystal-infilled photonic crystal. *Phys Rev E*. 2006;73:040701.
15. HH Li. Refractive Index of silicon and germanium and its wavelength and temperature derivatives. *J Phys Chem Ref Data*. 1980;9:561-658.
16. Suthar B, Bhargava A. Tunable multi-channel filtering using 1-D photonic quantum well structures. *Prog Electromagn Res Lett*. 2011;27:43-51.
17. Bhargava A, Suthar B. Localized modes in chalcogenide photonic multilayers with As-S-Se defect layer. *Chalcogen Lett*. 2009;6(10):529-533.
18. Schneider GJ, Watson GH. Nonlinear optical spectroscopy in one-dimensional photonic crystals. *Appl Phys Lett*. 2003;83:5350-5352.
19. Suthar B, Bhargava A. Improving the optical tuning and spectral efficiency in chalcogenide photonic quantum well structures. *J Ovonic Res*. 2010;6(3):117-123.
20. Kumar V, Singh KS, Ojha SP. Abnormal behaviour of one-dimensional photonic crystal with defect. *Optik*. 2011;122:1183-1187.
21. Kumar V, Singh KS, Ojha SP. Enhanced omnidirectional reflection frequency range in Si-based one dimensional photonic crystal with defect. *Optik*. 2011;122:910-913.
22. Suthar B, Nagar AK, Bhargava A. Tuning the localized mode in point defect chalcogenide photonic crystal. *Chalcogenide Lett*. 2009;6(11):623-627.
23. Suthar B, Nagar AK, Bhargava A. Slow light transmission in chalcogenide photonic crystal waveguide. *J Electron Sci Technol*. 2010;8(1):39-42.
24. Lee HY, Yao T. Design and evaluation of omnidirectional one-dimensional photonic crystals. *J Appl Phys*. 2003;93:819-837.
25. Jiang ZM, Shi, Zhao DT, Liu J, Wang. Silicon-based photonic crystal heterostructure. *Appl Phys Lett*. 2001;79:3395-3397.
26. Zhou WD, Sabarinathan J, Bhattacharya P, Kochman B, Berg EW, Yu, PC Pang SW. Characteristics of a photonic bandgap single defect microcavity electroluminescent device. *IEEE: J Quantum Electron*. 2001;(37):1153-1160.
27. Feise MW, Shadrivov IV, Kivshar YS. Bistable diode action in left-handed periodic structures. *Phys Rev E*. 2005;71:037602.
28. Hung HC, Wu CJ, Chang SJ. Terahertz temperature-dependent defect mode in a semiconductor-dielectric photonic crystal. *J Appl Phys*. 2011;110:093110.
29. Chang YH, Jhu YY, Wu. Temperature dependence of defect mode in a defective photonic crystal. *Opt Commun*. 2012;285(6):1501-1504.
30. Yeh P. *Optical Waves in Layered Media*. John Wiley and Sons, New York; 1988.
31. Born M, Wolf E. *Principle of Optics*. 4th edition, Pergamon, Oxford; 1970.
32. Ghosh. *Handbook of thermo-optic coefficients of optical materials with applications*. Academic Press, San Diego, CA, USA; 1997.
33. Kumar V, Suthar B, Kumar A, Singh KS, Bhargava A. The effect of temperature and angle of incidence on photonic band gap in a dispersive Si-based one dimensional photonic crystal. *Physica B*. 2013;416:106-109.

© 2014 Jindal et al.; This is an Open Access article distributed under the terms of the Creative Commons Attribution License (<http://creativecommons.org/licenses/by/3.0>), which permits unrestricted use, distribution, and reproduction in any medium, provided the original work is properly cited.

Peer-review history:
The peer review history for this paper can be accessed here:
<http://www.sciencedomain.org/review-history.php?iid=283&id=4&aid=2213>